

# Combined fast selective reduction using Mn-based catalysts and nonthermal plasma for NO<sub>x</sub> removal

Jun Xiang Chen<sup>1</sup> · Kuan Lun Pan<sup>1</sup> · Sheng Jen Yu<sup>2</sup> · Shaw Yi Yen<sup>2</sup> · Moo Been Chang<sup>1</sup>

Received: 11 March 2017 / Accepted: 19 July 2017 / Published online: 26 July 2017  
© Springer-Verlag GmbH Germany 2017

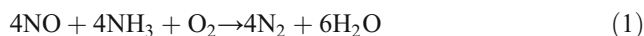
**Abstract** In this study, the concept of fast SCR for NO reduction with NH<sub>3</sub> as reducing agent is realized via the combination of nonthermal plasma (NTP) with Mn-based catalyst. Experimental results indicate that 10% wt. Mn-Ce-Ni/TiO<sub>2</sub> possesses better physical and chemical properties of surface, resulting in higher NO removal efficiency if compared with 10% wt. Mn-Ce/TiO<sub>2</sub> and 10% wt. Mn-Ce-Cu/TiO<sub>2</sub>. Mn-Ce-Ni/TiO<sub>2</sub> of 10% wt. achieves 100% NO<sub>x</sub> conversion at 150 °C, while 10% wt. Mn-Ce/TiO<sub>2</sub> and 10% wt. Mn-Ce-Cu/TiO<sub>2</sub> need to be operated at a temperature above 200 °C for 100% NO<sub>x</sub> conversion. However, NO conversion achieved with 10% wt. Mn-Ce-Ni/TiO<sub>2</sub> is significantly reduced as H<sub>2</sub>O<sub>(g)</sub> and SO<sub>2</sub> are introduced into the SCR system simultaneously. Further, two-stage system (SCR with DBD) is compared with the catalyst-alone for NO<sub>x</sub> conversion and N<sub>2</sub> selectivity. The results indicate that 100% NO<sub>x</sub> conversion can be achieved with two-stage system at 100 °C, while N<sub>2</sub> selectivity reaches 80%. Importantly, NO<sub>x</sub> conversion achieved with two-stage system could maintain >95% in the presence of C<sub>2</sub>H<sub>4</sub>, CO, SO<sub>2</sub>, and H<sub>2</sub>O<sub>(g)</sub>, indicating that two-stage system has better tolerance for complicated gas composition. Overall, this study demonstrates that combining NTP with Mn-based catalyst is effective in reducing NO<sub>x</sub> emission at a

low temperature (≤200 °C) and has good potential for industrial application.

**Keywords** Nitrogen oxides (NO<sub>x</sub>) · Selective catalytic reduction (SCR) · Nonthermal plasma (NTP) · Plasma catalysis

## Introduction

Continuous emission of large quantity of NO<sub>x</sub> into atmosphere has caused various environmental problems, such as acid rain, photochemical smog, and visibility degradation. Also, it is harmful to human health. Several post-combustion methods including selective catalyst reduction (SCR), selective non-catalyst reduction (SNCR), and non-selective catalyst reduction (NSCR) are available to control NO<sub>x</sub> emissions. Among them, selective catalyst reduction (SCR) is of the highest NO<sub>x</sub> removal efficiency and NH<sub>3</sub> is commonly applied as a reducing agent to reduce NO<sub>x</sub> to form N<sub>2</sub> in the presence of O<sub>2</sub> (Jun et al. 2015). Generally, NO<sub>x</sub> removal efficiency achieved with SCR process could reach 90% if appropriate catalyst is applied (Wu et al. 2007). The main reaction of SCR is described as rReaction (1).



V<sub>2</sub>O<sub>5</sub>-WO<sub>3</sub>/TiO<sub>2</sub> is typically used in SCR process; however, it needs to be operated within the temperature range of 250–350 °C for high efficiency. The narrow reaction temperature window is considered as one of the main disadvantages of SCR. In addition, the catalyst deactivation always takes place, because SCR catalyst is generally placed before particle removal equipment and flue gas desulfurization (FGD) (Phil et al. 2008). Also, SCR process shows good efficiency for

Responsible editor: Suresh Pillai

✉ Moo Been Chang  
mbchang@ncuen.ncu.edu.tw

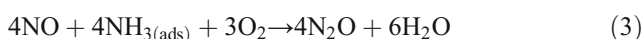
<sup>1</sup> Graduate Institute of Environmental Engineering, National Central University, No.300, Jhongda Road, Jhongli District, Taoyuan City 32001, Taiwan

<sup>2</sup> Green Energy and Environment Institute, Industrial Technology Research Institute, Hsinchu, Taiwan

NO<sub>x</sub> removal with urea as a reducing agent for the treatment of flue gas from diesel engine (Choi and Woo 2015; Cimino et al. 2016). Urea has several advantages such as easier transportation, higher safety of storage, and higher stability if compared with NH<sub>3</sub> (Feng and Lü 2015). However, the temperature of low-loading diesel engine exhaust is relatively low (100–200 °C). As mentioned previously, the most disadvantage of applying SCR in controlling diesel emission is that the catalysts have to be operated at a temperature higher than 200 °C. As a result, conventional SCR could not be applied for removing NO<sub>x</sub> from diesel engine exhaust (Chen et al. 2016; Yoshida et al. 2012). Therefore, how to develop a low-temperature SCR has become an emerging issue. Recently, relevant study indicated that SCR catalyst has good potential to convert the NO<sub>x</sub> to N<sub>2</sub> at lower temperatures; further, it can be placed downstream of the particle control device such as bag filter and the desulfurization system to avoid the deactivation of catalyst (Huang et al. 2016).

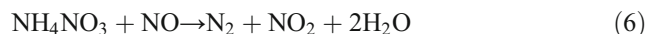
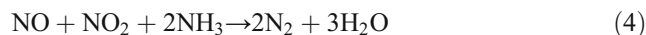
Manganese-based (Mn-based) catalysts such as MnO<sub>x</sub>, MnO<sub>x</sub>/TiO<sub>2</sub> (Jin et al. 2014), Mn-Ce/TiO<sub>2</sub> (Cao et al. 2015), and Mn-Ce-Fe/γ-Al<sub>2</sub>O<sub>3</sub> (Thirupathi and Smirniotis 2011a) have attracted much attention due to their high capability in converting NO<sub>x</sub> at low temperatures (≤200 °C). Previous studies indicated that applying different metals as promoters can enhance the activity of Mn-based catalyst, such as Ce, Cu, Fe, and Ni. Especially Ce is most applied for developing low-temperature catalysts (Liu et al. 2017). Kwon et al. (2015) reported that Ce has good activity toward NO<sub>x</sub> reduction due to its redox properties. Additionally, Ce could store and release oxygen via the transformation between Ce<sup>4+</sup> and Ce<sup>3+</sup> to promote SCR reaction (Kwon et al. 2015). Zhou et al. (2016) investigated Ce-based catalysts with different Ce valences (Zhou et al. 2016) and indicated that catalyst has a higher sulfur dioxide resistance as the ratio of Ce<sup>4+</sup>/(Ce<sup>4+</sup>+Ce<sup>3+</sup>) is increased. Thirupathi et al. (2011) indicated that activity of Mn-based catalyst can be promoted by adding Ni for SCR process, because Ni can also enhance redox capacity of catalyst (Thirupathi and Smirniotis 2011b).

However, Mn-based catalysts still face serious drawbacks although it has potential to be operated at a lower temperature for SCR process (Yang et al. 2016). For example, N<sub>2</sub>O is the inevitable product in a low-temperature SCR process, resulting in a lower N<sub>2</sub> selectivity. Niu et al. (2016) indicated that N<sub>2</sub>O may be generated from direct oxidation of NH<sub>3</sub> in the excess O<sub>2</sub> via reaction (2) at a low temperature (≤150 °C) or NO would react with adsorbed NH<sub>3</sub> on catalyst surface via reaction (3) (Niu et al. 2016).



Similarly, Mn-based catalysts have poor durability and resistance in complicated gas composition (especially in the

presence of SO<sub>2</sub> and H<sub>2</sub>O<sub>(g)</sub>); Mn-based catalysts could be seriously poisoned by formation of ammonia bisulfate (NH<sub>4</sub>HSO<sub>4</sub> and (NH<sub>4</sub>)<sub>2</sub>SO<sub>4</sub>) on the catalyst. On the other hand, SCR performance could be significantly enhanced as fast-SCR is applied. Especially, fast-SCR is effective to reduce NO to N<sub>2</sub> at a low temperature. Generally, fast-SCR has a higher reaction rate and wider reaction temperature window if compared with conventional SCR. Fast-SCR was first investigated by Koebel et al. (2001, 2002) and Madia et al. (2002) and can be described as reaction (4). Relevant study indicated that redox mechanism in fast-SCR is similar to the standard SCR reaction (Grossale et al. 2008). For fast-SCR process, NO<sub>2</sub> plays a crucial role which serves as a more efficient oxidizing agent than O<sub>2</sub> in the redox process of the SCR reaction. In fast-SCR, NH<sub>4</sub>NO<sub>3</sub> is formed via the reaction between NH<sub>3</sub> and NO<sub>2</sub>, and subsequently, NH<sub>4</sub>NO<sub>3</sub> will be decomposed by NO described in reactions (5) and (6). Relevant study indicated that reactions (5) and (6) are closely related to the fast-SCR chemistry (Grossale et al. 2008). The vital process is the redox reactions as indicated in reactions (5) and (6), which dominate the reaction rate of fast-SCR. It has been proved that existence of NO<sub>2</sub> in the exhaust gas is essential and the content of NO<sub>2</sub> approximately equals to that of NO favors fast-SCR reaction (Iwasaki and Shinjoh 2010).



However, NO<sub>x</sub> in the typical flue gas of combustion system is composed of 95% NO and 5% NO<sub>2</sub>; therefore, fast-SCR process is difficult to be applied. How to effectively convert NO into NO<sub>2</sub> is an important step for fast-SCR process (Jögi et al. 2016; Kang et al. 2006a). Nonthermal plasma (NTP) has been demonstrated as an effective technology to oxidize NO into NO<sub>2</sub> or NO<sub>3</sub><sup>-</sup> via the collision with highly active radicals generated, i.e., O and OH (Patil et al. 2016). Combining catalyst with NTP to form plasma catalysis is a novel reaction system, which is regarded as feasible technology for reducing the emission of gaseous pollutants. Generally, plasma catalysis system can be distinguished into two configurations, i.e., in-plasma catalysis (IPC) and post-plasma catalysis (PPC). The former is similar to a packed-bed reactor, namely, catalyst is directly packed into the discharge zone. The latter implies that catalyst is located downstream NTP reactor, and catalysis system and plasma reactor are operated separately.

Bröer and Hammer (2000) reported that NO<sub>x</sub> conversion can reach 90% at 160 °C by combining dielectric barrier discharges (DBD) with V<sub>2</sub>O<sub>5</sub>-WO<sub>3</sub>/TiO<sub>2</sub> catalyst to form two-stage system (Bröer and Hammer 2000). Tran et al. (2004) applied DBD and In-doped γ-alumina catalyst to form a two-stage system for reducing of NO<sub>x</sub> and indicated that 100% NO<sub>x</sub> conversion could be achieved at 350 °C (Tran

et al. 2004). Cho et al. (2012) also applied plasma to assist the HC-SCR and indicated that  $\text{NO}_x$  conversion reached 100% with the operating temperature of 300 °C and applied voltage of 16 kV (Cho et al. 2012). Hence, PPC has good potential to reduce the emission of  $\text{NO}_x$ .

As mentioned previously, Mn-based catalysts have potential to be applied for  $\text{NO}_x$  reduction at a temperature below 200 °C. The aim of this study is to develop low-temperature SCR catalysts through various Mn-modified catalysts, which are Mn-Ce/ $\text{TiO}_2$ , Mn-Ce-Ni/ $\text{TiO}_2$ , and Mn-Ce-Cu/ $\text{TiO}_2$ , respectively. Additionally, a lab-scale two-stage system consisting of NTP and low-temperature SCR catalysts is developed to reduce NO from simulated gas streams. In this two-stage system, NTP can be regarded as an oxidation system to achieve  $\text{NO}_2/\text{NO} \approx 1$ . It is expected that combining Mn-based catalyst with plasma would enhance  $\text{NO}_x$  conversion and reduce the formation of  $\text{N}_2\text{O}$ . Furthermore, the effects of operating parameters on  $\text{NO}_x$  removal efficiency are extensively evaluated via a lab-scale experimental setup, and gas streams with complicated gas compositions are applied to evaluate the practical application of this two-stage system for NO removal.

## Experimental

### Catalyst preparation

A series of Mn-based catalysts including 10% wt. Mn-Ce/ $\text{TiO}_2$ , 10% wt. Mn-Ce-Ni/ $\text{TiO}_2$ , and 10% wt. Mn-Ce-Cu/ $\text{TiO}_2$  were prepared by wet impregnation method. First of all, corresponding metal nitrates (including  $\text{Mn}(\text{NO}_3)_2 \cdot 4\text{H}_2\text{O}$  (purity: 98%, Showa),  $\text{Ce}(\text{NO}_3)_3 \cdot 6\text{H}_2\text{O}$  (purity: 99%, ACROS),  $\text{Ni}(\text{NO}_3)_2 \cdot 6\text{H}_2\text{O}$  (purity: 99%, Showa), and  $\text{Cu}(\text{NO}_3)_2 \cdot 3\text{H}_2\text{O}$ , (purity: 100%, Showa) as precursors were dissolved in deionized water to prepare aqueous solution with appropriate stoichiometry. All ratios of active phases of catalysts (i.e., Mn-Ce, Mn-Ce-Ni, and Mn-Ce-Cu) were controlled at 1. Subsequently, corresponding P25-type  $\text{TiO}_2$  (purity: 100%, Degussa) used as support was added into mixture solution and mixed completely at 80 °C until water was evaporated. Secondly, the residual solid precursor was placed into an oven to dry overnight, and then calcined in air at 400 °C for 4 h with the heating rate of 5 °C/min. Finally, all catalysts were sieved to 30–70 mesh for catalytic test.

### Catalyst characterization

The crystal structures of catalysts were characterized by powder X-ray diffraction (XRD). The XRD (D8AXRD BRUKER, Germany) profiles were obtained using an X-ray diffractometer, operated at 40 kV and 40 mA using Cu-K $\alpha$  radiation with a nickel filter, diffraction with  $2\theta$  were recorded over the range of 10–80°. The specific surface areas, total pore

volume, and average pore diameter of the catalysts were measured by  $\text{N}_2$  adsorption at –196 °C with a Micromeritics ASAP 2010 (ASAP2010 Micromeritics, USA). Field-emission scanning electron microscopy (FE-SEM) equipped with an energy-dispersive X-ray spectroscopy (EDS) was used to examine the micro-structure of catalyst surface and the elemental composition of catalysts by S80 JEOL (SEM, S80 JEOL, Japan). X-ray photoelectron spectroscopy (XPS, Sigma Probe VG, UK) was used to analyze the chemical state of elements of the catalysts, and XPS spectra were recorded with monochromatic Al anode X-ray which was equipped with a concentric hemispherical analyzer. Al K $\alpha$  (1486.6 eV) X-ray source was used for excitation. The binding energies were referenced to the C1s line at 284.5 eV. Thermogravimetric analysis (TGA, Pyris 1 TGA PERKIN ELMER, USA) was carried out to investigate the thermal stability of sulfate species in a static  $\text{N}_2$  atmosphere, with Hitachi STA7300. The TGA experiments were conducted with 10–20-mg catalysts, and it was analyzed with the temperature ranging from room temperature to 900 °C at a rate of 10 °C/min.

### Activity test

Low-temperature reduction of NO with ammonia was first performed with SCR process at a fixed-bed quartz reactor (I.D.= 20 mm) containing 6 g catalyst in excess oxygen. The SCR process was carried out with the temperature ranging from 50 to 200 °C and the total gas flow rate was fixed at 1500 sccm, corresponding to a gas hourly space velocity (GHSV) of 20,000  $\text{h}^{-1}$ . Typical gas mixture consisted of  $\text{NO} = 300$  ppm,  $\text{NH}_3 = 300$  ppm,  $\text{O}_2 = 10\%$ ,  $\text{H}_2\text{O}_{(\text{g})} = 10\%$  (when used),  $\text{SO}_2 = 100$  ppm (when used), and  $\text{N}_2$  as balance. Various gases were provided by gas cylinders and a set of mass flow controllers (MFC) were used for regulating the gas flow rates, while  $\text{H}_2\text{O}_{(\text{g})}$  was introduced into the system by a peristaltic pump. For the analysis of exhaust, a condensation system was used to capture  $\text{H}_2\text{O}_{(\text{g})}$  in order to avoid the damage to instruments. An  $\text{NO}_x$  analyzer (Testo 350, Germany) was used to measure NO and  $\text{NO}_2$  concentrations while  $\text{N}_2\text{O}$  was analyzed by Fourier transform infrared spectrophotometer (FTIR, Nicolet 6700 Thermo Scientific, USA).

Further, the two-stage system was constituted by combining DBD-type (dielectric barrier discharge) NTP with Mn-based catalyst, and it was evaluated for the effectiveness in removing  $\text{NO}_x$ . As shown in Fig. 1, the catalysis system (SCR process) was placed downstream of the NTP (similar to PPC system). Likewise, the total gas flow rate of two-stage system was controlled at 1500 sccm. In two-stage system, all operating conditions were similar to SCR process. For NTP system, the DBD-type reactor was constituted of a quartz tube (I.D. = 10 mm) filled with glass beads, a stainless steel rod,

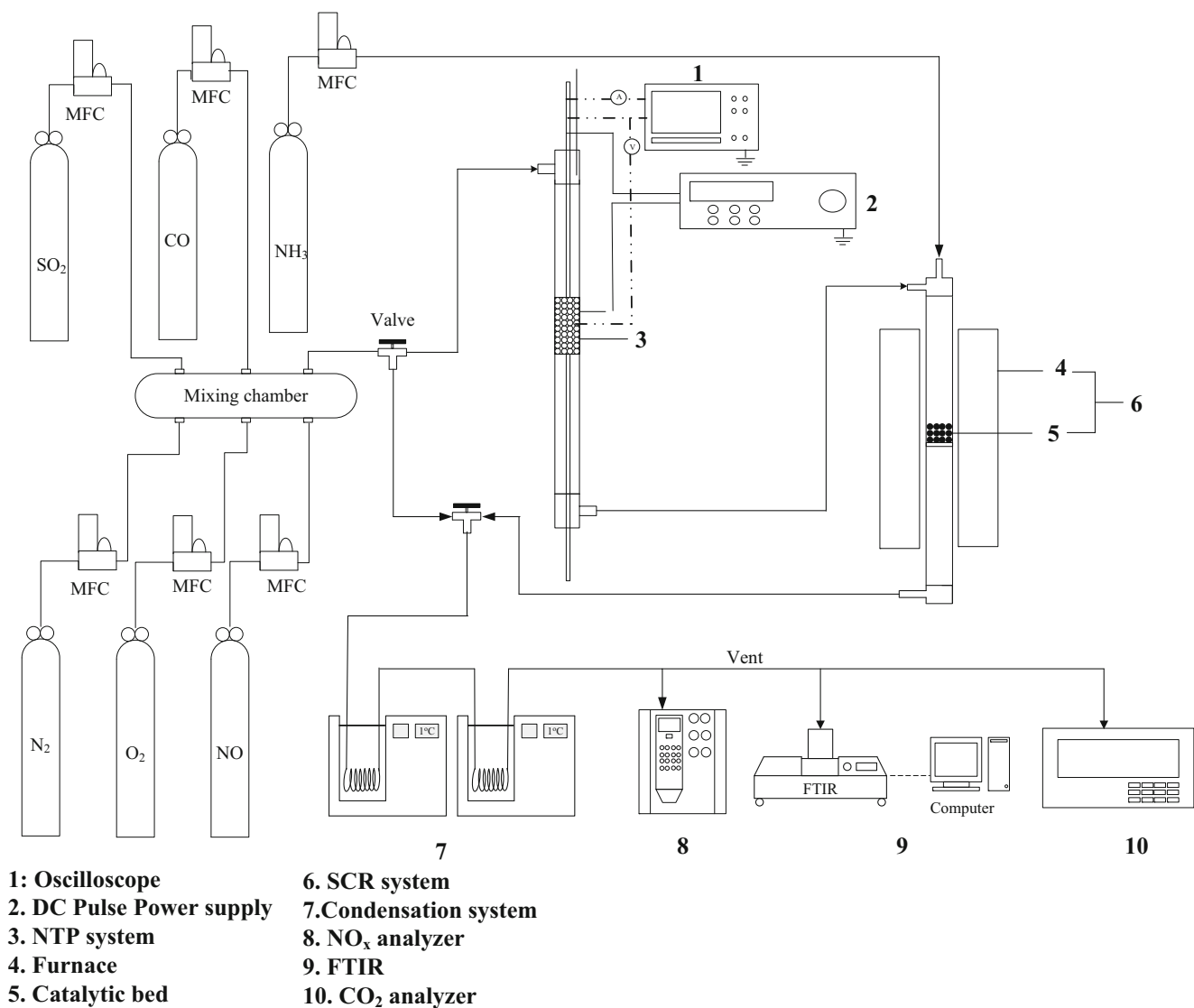


Fig. 1 Schematic of the two-stage system for NO<sub>x</sub> reduction

and a stainless steel wire mesh, where stainless steel rod and a stainless steel wire mesh were used as the inner and outer electrodes, respectively. The operating temperature and pressure of NTP were 25 °C and atmospheric pressure, respectively. The DC pulse power was applied to generate plasma, and the applied voltage and frequency were controlled at 12–20 kV and 8–10 kHz, respectively, for test. The discharge power was measured by a digital oscilloscope equipped with a current probe and a high-voltage probe. The NO<sub>x</sub> conversion and N<sub>2</sub> selectivity are calculated via Eqs. (7) and (8), respectively:

$$NO \text{ conversion}(\%) = \frac{[NO]_{in} - [NO]_{out}}{[NO]_{in}} \times 100(\%) \quad (7)$$

$$SN_2 = \frac{[NO]_{in} - [NO]_{out} - [NO_2] - 2[N_2O]}{[NO]_{in} - [NO]_{out}} \times 100\% \quad (8)$$

## Results and discussion

### Catalyst characterizations—XRD, BET, and SEM

The XRD patterns of Mn-Ce/TiO<sub>2</sub>, Mn-Ce-Ni/TiO<sub>2</sub>, and Mn-Ce-Cu/TiO<sub>2</sub> are presented in Fig. 2, and the result indicates that all catalysts prepared present strong diffraction peaks of TiO<sub>2</sub>, being mainly contributed by anatase crystalline. It is observed that three Mn-based catalysts have basically amorphous peaks of MnO<sub>x</sub> on the catalyst surface. Previous studies reveal that amorphous MnO<sub>2</sub> is of higher activity if compared with crystalline MnO<sub>2</sub> for NO reduction (Boningari et al. 2015; Tang et al. 2007). The presence of amorphous manganese oxide in Mn-based catalysts may be one of the key factors for their excellent activities in removing NO<sub>x</sub> (Kang et al. 2006b; Peña et al. 2004). In addition, Cu and Ni are not

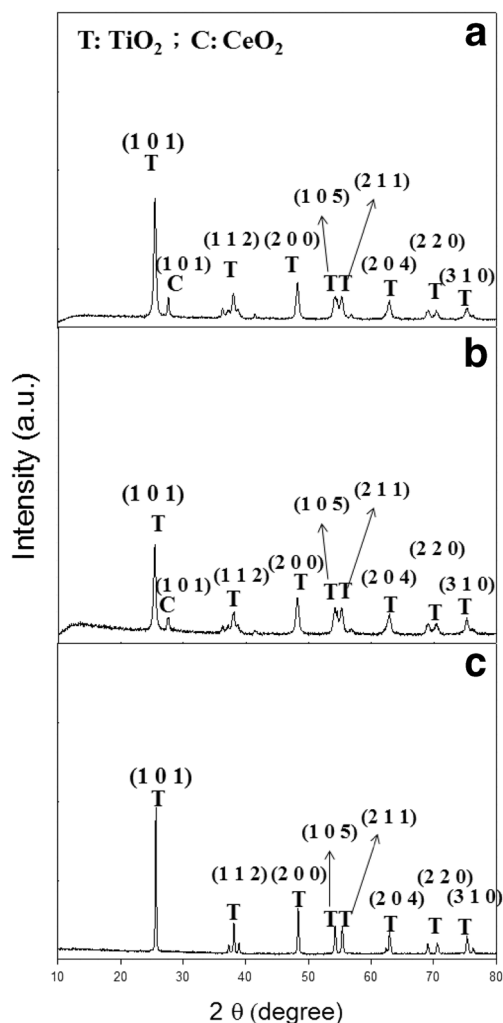


**Fig. 2** XRD patterns of Mn-based catalysts. **a** Mn-Ce-Ni/TiO<sub>2</sub>. **b** Mn-Ce/TiO<sub>2</sub>. **c** Mn-Ce-Cu/TiO<sub>2</sub>

observed in XRD profiles of Mn-Ce-Cu/TiO<sub>2</sub> and Mn-Ce-Ni/TiO<sub>2</sub>, respectively. It is speculated that they may be incorporated into Mn lattice to form solid solution. The diffraction peaks of CeO<sub>2</sub> are not present in Mn-Ce-Cu/TiO<sub>2</sub> due to less Ce content. As shown in EDS results (see Table 1), Mn-Ce-Cu/TiO<sub>2</sub> has lower contents of Cu, Mn, and Ce, and it is speculated that active phase (Mn-Ce-Cu) is not well supported on TiO<sub>2</sub> due to the addition of Cu.

The specific surface areas ( $S_{\text{BET}}$ ), average pore diameter, and pore volume of catalysts and TiO<sub>2</sub> are summarized in Table 2.

**Table 1** Elemental compositions of the catalysts prepared

| Catalyst                  | EDS (atomic %) |      |      |      |       |       |
|---------------------------|----------------|------|------|------|-------|-------|
|                           | Mn             | Ce   | Ni   | Cu   | Ti    | O     |
| Mn-Ce/TiO <sub>2</sub>    | 4.31           | 5.04 | –    | –    | 55.26 | 35.39 |
| Mn-Ce-Ni/TiO <sub>2</sub> | 4.22           | 4.27 | 4.06 | –    | 50.03 | 37.42 |
| Mn-Ce-Cu/TiO <sub>2</sub> | 3.24           | 3.28 | –    | 3.33 | 61.05 | 29.10 |

The results indicate that BET surface areas of Mn-Ce/TiO<sub>2</sub>, Mn-Ce-Ni/TiO<sub>2</sub>, and Mn-Ce-Cu/TiO<sub>2</sub> are 48, 50, and 30 m<sup>2</sup>/g, respectively. Obviously, BET surface areas of catalysts prepared decrease as TiO<sub>2</sub> is impregnated with various metal elements. Possibly, parts of TiO<sub>2</sub> pores are covered. Also, it is found that pore volume of TiO<sub>2</sub> decreases to some extent after impregnation. Among Mn-based catalysts, Mn-Ce-Ni/TiO<sub>2</sub> shows the largest BET (~50 m<sup>2</sup>/g) and average pore diameter (8.6 nm), and it may correspond to the highest activity due to smaller diffusion limitation. As shown in Table 1, EDS analysis indicates that the elemental composition of the catalysts prepared deviates a little from the designated formula of catalysts. In addition, it is observed that Mn-Ce-Ni/TiO<sub>2</sub> has the highest oxygen content among three catalysts prepared. According to SCR mechanism, NH<sub>3</sub> is first adsorbed on reactive oxygen of catalyst. Hence, it is speculated that higher oxygen atom content may result in higher NO conversion. Figure 3 displays the SEM images of Mn-Ce-Ni/TiO<sub>2</sub>, Mn-Ce/TiO<sub>2</sub>, and Mn-Ce-Cu/TiO<sub>2</sub>, respectively. The results reveal that three Mn-based catalysts are mainly constituted by pseudo-spherical particles; they are composed of irregular small particles corresponding to the prepared method. The average particle sizes of 3 Mn-based catalysts were calculated by Sherr's equation, and their particle sizes are Mn-Ce-Ni/TiO<sub>2</sub> = 25 nm, Mn-Ce/TiO<sub>2</sub> = 28 nm, and Mn-Ce-Cu/TiO<sub>2</sub> = 31 nm, respectively. The particle sizes of catalysts rank in the order of Mn-Ce-Cu/TiO<sub>2</sub> > Mn-Ce/TiO<sub>2</sub> > Mn-Ce-Ni/TiO<sub>2</sub>. Especially, Mn-Ce-Cu/TiO<sub>2</sub> reveals severe sintering after calcination (see Fig. 3), resulting in lower BET (30 m<sup>2</sup>/g). On the other hand, sintering of Mn-Ce-Ni/TiO<sub>2</sub> is not significant if compared with Mn-Ce/TiO<sub>2</sub> and Mn-Ce-Cu/TiO<sub>2</sub>. Previous study indicated that addition of Ni to Mn-based catalysts can prevent its sintering, and higher catalytic activity is obtained (Thirupathi et al. 2011). Overall, Mn-Ce-Ni/TiO<sub>2</sub> presents better surface characteristics if compared with Mn-Ce/TiO<sub>2</sub> and Mn-Ce-Cu/TiO<sub>2</sub>.

## SCR performance

### Low-temperature SCR performance

Catalytic activities of three Mn-based catalysts prepared are first evaluated for NH<sub>3</sub>-SCR reaction at various temperatures.

**Table 2** BET, pore diameter, and pore volume of TiO<sub>2</sub> and three Mn-based catalysts

| Catalyst                  | BET (m <sup>2</sup> /g) | Average pore diameter (nm) | Pore volume (cm <sup>3</sup> /g) |
|---------------------------|-------------------------|----------------------------|----------------------------------|
| TiO <sub>2</sub>          | 60                      | 6.8                        | 0.36                             |
| Mn-Ce/TiO <sub>2</sub>    | 48                      | 7.8                        | 0.30                             |
| Mn-Ce-Ni/TiO <sub>2</sub> | 50                      | 8.6                        | 0.28                             |
| Mn-Ce-Cu/TiO <sub>2</sub> | 30                      | 8.0                        | 0.25                             |

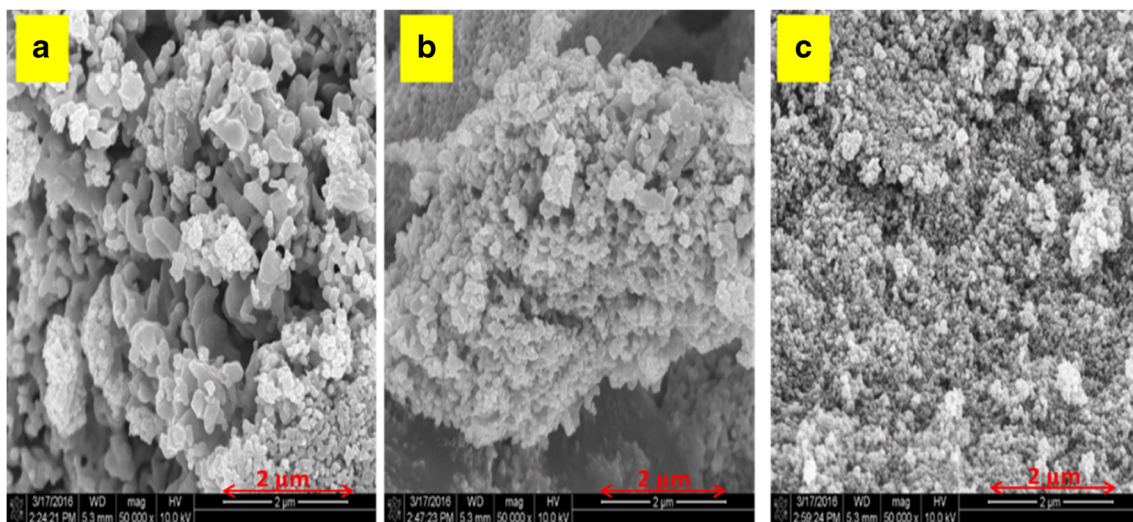


**Fig. 3** SEM images of Mn-based catalysts. **a** Mn-Ce-Ni/TiO<sub>2</sub>. **b** Mn-Ce/TiO<sub>2</sub>. **c** Mn-Ce-Cu/TiO<sub>2</sub>

As shown in Fig. 4, the NO<sub>x</sub> conversions achieved increase with increasing temperature for three Mn-based catalysts. At 50 °C, NO<sub>x</sub> conversion achieved with Mn-Ce-Ni/TiO<sub>2</sub>, Mn-Ce/TiO<sub>2</sub>, and Mn-Ce-Cu/TiO<sub>2</sub> are 58, 31, and 30%, respectively. As temperature is increased to 150 °C, NO<sub>x</sub> conversions achieved with Mn-Ce-Ni/TiO<sub>2</sub> and Mn-Ce/TiO<sub>2</sub> reach 100% while Mn-Ce-Cu/TiO<sub>2</sub> needs to be operated at 200 °C for reaching 95% NO<sub>x</sub> conversion. Activities of three Mn-based catalysts for NO reduction rank in the order of Mn-Ce-Ni/TiO<sub>2</sub> > Mn-Ce/TiO<sub>2</sub> > Mn-Ce-Cu/TiO<sub>2</sub>. For the effect of Ni on activity of Mn-based catalyst, previous study indicated that Mn/TiO<sub>2</sub> has positive interaction if doped with Ni (Thirupathi et al. 2011). This interaction may lead to the enhancement of the oxygen mobility, resulting in higher activity for SCR process.

Additionally, the kinetics is investigated by the power rate law model. The activation energies are calculated on the basis of the conversion smaller than 20% by increasing GHSV. The kinetics study is conducted by assuming steady-state before

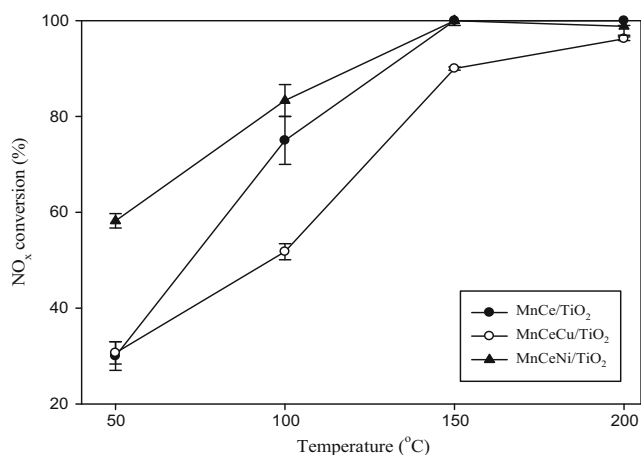


**Fig. 4** The performance of three Mn-based catalysts (NO: 300 ppm, NH<sub>3</sub>: 300 ppm, O<sub>2</sub>: 10%, balance: N<sub>2</sub> and GHSV = 20,000 h<sup>-1</sup>)

and after reaction, and a mathematical model of a differential-type reactor is used for determining the reaction rates ( $-r_i$ ) at different temperatures (T) and inlet NO concentrations ( $C_i$ ). Subsequently, regression straight lines of  $1/r_i$  versus  $1/C_i$  are plotted to obtain the values of rate constant ( $k$ ) with different temperatures. Then, a regression line is obtained by plotting  $\ln k$  versus  $1/T$ , and activation energy ( $E_a$ ) is calculated by Arrhenius equation (see Fig. 5). The result indicates that activation energy with Mn-Ce-Ni/TiO<sub>2</sub> as catalyst for SCR process is 23.1 kJ/mol.

*XPS analysis of catalysts*

XPS spectra are used to understand the chemical bonding states on the catalyst surface for analysis of mechanism. XPS Mn 2p spectra of three fresh catalysts are presented in Fig. 6a. For all three catalysts, two main peaks corresponding to Mn 2p<sub>3/2</sub> and Mn 2p<sub>1/2</sub> are located at 642 and 653 eV, respectively. Among them, Mn 2p<sub>3/2</sub> can be separated into

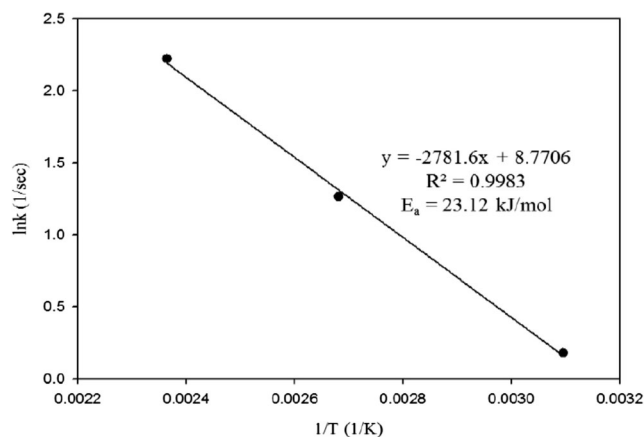


**Fig. 5** Arrhenius plot for rate constant of NO conversion with Mn-Ce-Ni/TiO<sub>2</sub> as catalyst

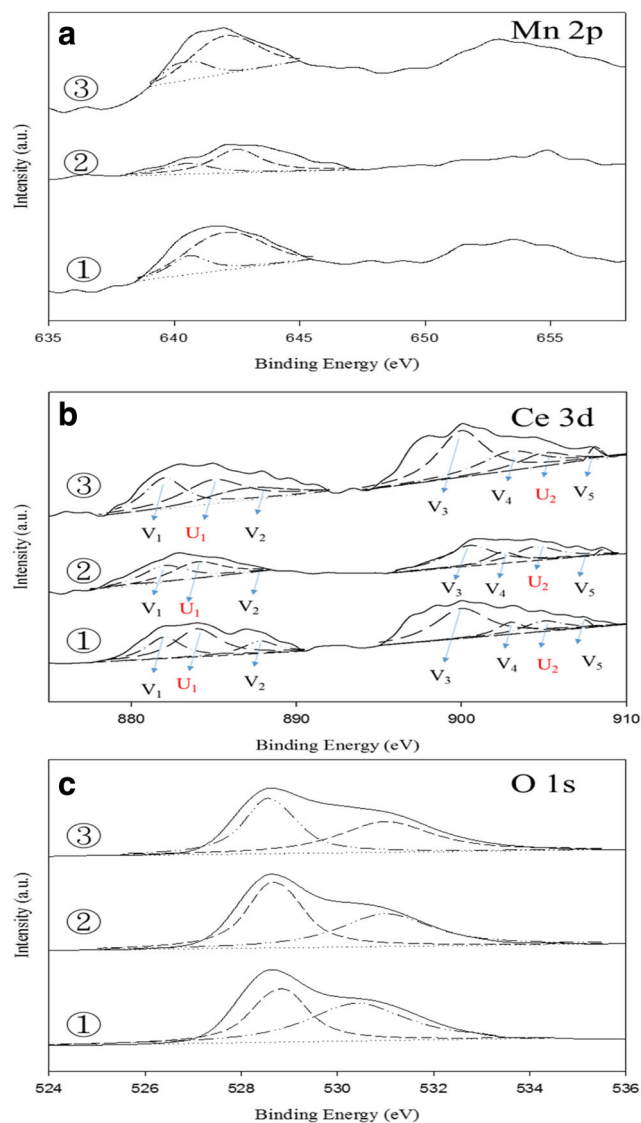


**Fig. 6** XPS analysis of three catalysts. **a** Mn 2p. **b** Ce 3d. **c** O 1s (① MnCeNi/TiO<sub>2</sub>, ② MnCe/TiO<sub>2</sub>, ③ MnCeCu/TiO<sub>2</sub>)

two peaks, corresponding to Mn<sup>4+</sup> (642.0–642.5 eV) and Mn<sup>3+</sup> (641.0–641.3 eV), respectively (Chang et al. 2013; Shaju et al. 2002).

Figure 6b shows the valence state of Ce 3d of three catalysts. The Ce 3d peaks were fitted into the sub-bands, and those marked as U<sub>1</sub> and U<sub>2</sub> represent Ce<sup>+3</sup> species. The sub-bands marked as V<sub>1</sub>, V<sub>2</sub>, V<sub>3</sub>, V<sub>4</sub>, and V<sub>5</sub> are attributed to Ce<sup>4+</sup> species. In addition, XPS spectra of the O 1s of three Mn-based catalysts are presented in Fig. 6c. The results indicate that the two main peaks appeared at 529–530 and 531–532 eV, corresponding to lattice oxygen (O<sub>β</sub>) and adsorbed surface oxygen (O<sub>α</sub>), respectively (Peng et al. 2013).

Fang et al. (2015) indicated that Mn<sup>4+</sup> has a higher activity than Mn<sup>3+</sup> and Mn<sup>2+</sup> toward NO<sub>x</sub> removal (Fang et al. 2015). Wang et al. (2016) mentioned that Mn<sup>4+</sup> species could enhance the oxidation of NO to NO<sub>2</sub>, further promote SCR

performance at a low temperature (Wang et al. 2016). Wan et al. (2014) indicated that the surface Mn<sup>4+</sup> species is the predominant valence state of the Mn-based catalysts and the activity of Mn-based catalysts increases with increasing Mn<sup>4+</sup>. To summarize above results, Mn<sup>4+</sup> has better electron mobility and thus higher production of oxygen defect (Wan et al. 2014). Regarding the effect of Ce, previous study indicated that the activity of SCR catalyst increases with increasing Ce<sup>4+</sup>/(Ce<sup>4+</sup>+Ce<sup>3+</sup>) ratio. As shown in Fig. 6c, O 1s of three catalysts have two peaks, which are O<sub>β</sub> and O<sub>α</sub>, respectively. Relevant study indicated that the catalyst activity is related to ratio of O<sub>α</sub>/(O<sub>α</sub> + O<sub>β</sub>) in SCR process (Shu et al. 2014). Generally, O<sub>α</sub> has a higher mobility than O<sub>β</sub>, leading to the enhancement of SCR catalytic activity (Ma et al. 2015). Indeed, the results of three Mn-based catalyst are similar to that reported in literature, and the ratios of Mn<sup>4+</sup>/(Mn<sup>4+</sup>+Mn<sup>3+</sup>), Ce<sup>4+</sup>/(Ce<sup>4+</sup>+Ce<sup>3+</sup>), and O<sub>α</sub>/(O<sub>α</sub> + O<sub>β</sub>) of three catalysts are summarized at Table 3. Mn-Ce-Ni/TiO<sub>2</sub> reveals the best SCR performance of three catalysts, and it also has the highest Mn<sup>4+</sup>/(Mn<sup>4+</sup>+Mn<sup>3+</sup>), Ce<sup>4+</sup>/(Ce<sup>4+</sup>+Ce<sup>3+</sup>), and O<sub>α</sub>/(O<sub>α</sub> + O<sub>β</sub>) ratios. Previous study indicated that addition of Ni to Mn-based catalyst improves surface properties of Mn-based catalyst, resulting in better catalysis, because Ni has good interaction with Mn and Ti (Thirupathi et al. 2011). Conversely, the performance of Mn-Ce-Cu/TiO<sub>2</sub> decreases due to weak or no interaction of Cu with Ti (Bocuzzi et al. 1997). The results indicate that Ni is a good promoter, and it could increase the formation of Mn<sup>4+</sup>, resulting in higher SCR performance. With the addition of nickel into Mn-Ce/TiO<sub>2</sub> catalyst, the ratio of Mn<sup>4+</sup>/(Mn<sup>4+</sup>+Mn<sup>3+</sup>) increases from 72 to 79%. Obviously, the activity of Mn-Ce/TiO<sub>2</sub> is significantly improved by modification with Ni. Experimental results indicate that Mn-Ce-Ni/TiO<sub>2</sub> has the highest activity on NO<sub>x</sub> reduction. Therefore, Mn-Ce-Ni/TiO<sub>2</sub> is mainly applied for further tests.

#### *Effect of SO<sub>2</sub> and H<sub>2</sub>O<sub>(g)</sub> on low temperature SCR*

As reported previously, Mn-Ce-Ni/TiO<sub>2</sub> catalyst is demonstrated with the highest activity in SCR process. The long-term activity is further investigated for NO<sub>x</sub> removal, and the results indicate that NO<sub>x</sub> conversion maintains above 99% in the time course over 80 h at 150 °C, indicating high stability of Mn-Ce-Ni/TiO<sub>2</sub> for NO reduction.

It is important to evaluate the effects of H<sub>2</sub>O<sub>(g)</sub> and SO<sub>2</sub> on the catalytic activity (Shen et al. 2014). Figure 7 illustrates the effects of 10% H<sub>2</sub>O<sub>(g)</sub> and 100 ppm SO<sub>2</sub> on SCR performance at 150 °C. The NO<sub>x</sub> conversion decreases from 100 to 80% as 100 ppm SO<sub>2</sub> and 10% H<sub>2</sub>O<sub>(g)</sub> are introduced into the gas stream simultaneously. As SO<sub>2</sub> and H<sub>2</sub>O<sub>(g)</sub> feedings are turned off, the NO<sub>x</sub> conversion gradually increases to 90%. These results indicate that the activity of Mn-Ce-Ni/TiO<sub>2</sub> could be inhibited as H<sub>2</sub>O<sub>(g)</sub> and SO<sub>2</sub> are simultaneously present in flue gas. Possibly, SO<sub>2</sub> are oxidized into SO<sub>3</sub> or sulfate species on

**Table 3** Percentages of different valence states for Mn and Ce of three catalysts

| Catalysts               | Mn <sup>4+</sup> /(Mn <sup>4+</sup> +Mn <sup>3+</sup> ) (%) | Ce <sup>4+</sup> /(Ce <sup>4+</sup> +Ce <sup>3+</sup> ) (%) | O <sub>α</sub> /(O <sub>α</sub> + O <sub>β</sub> ) (%) |
|-------------------------|---|---|--|
| MnCeNi/TiO <sub>2</sub> | 79  | 64  | 50   |
| MnCe/TiO <sub>2</sub>   | 72  | 61  | 30   |
| MnCeCu/TiO <sub>2</sub> | 64  | 59  | 46   |

MnO<sub>x</sub> during SCR process, then SO<sub>3</sub> or sulfate species move to Ce or Ni to form bulk-sulfate species. Yu et al. (2010) mentioned that the NO conversion can be recovered to 90%, being attributed to decomposition of adsorbed ammonium sulfate when H<sub>2</sub>O<sub>(g)</sub> and SO<sub>2</sub> are turned off (Yu et al. 2010).

To confirm SCR behaviors in the presence of SO<sub>2</sub> and H<sub>2</sub>O<sub>(g)</sub>, used Mn-Ce-Ni/TiO<sub>2</sub> catalysts were analyzed by thermogravimetric analysis. The sulfate species and H<sub>2</sub>O<sub>(g)</sub> adsorbed on the surface of catalysts would lead to weight increase. As shown in Fig. 8, the TGA curve presents three major weight losses for Mn-Ce-Ni/TiO<sub>2</sub>. The first one appears at 100 °C, which can be attributed to the evaporation of water. The second and third losses appear at approximately 400 and 800 °C, respectively, which are originated from the decomposition of sulfate species, such as NH<sub>4</sub>HSO<sub>4</sub> and (NH<sub>4</sub>)<sub>2</sub>SO<sub>4</sub> (Putluru et al. 2015).

**NO<sub>x</sub> reduction via two-stage system**

The system combining NTP and Mn-Ce-Ni/TiO<sub>2</sub> catalyst is evaluated for the effectiveness in reducing NO<sub>x</sub>. In order to elucidate the effects of NTP on catalytic performance, the gas compositions are kept the same as that listed in section “SCR performance.” The DBD experiment is conducted with the applied voltage of 15.5 kV and a frequency of 10,000 Hz to generate plasma. The NO and NO<sub>2</sub> concentrations after plasma are measured as 165 and 153 ppm, respectively, and the ratio of NO<sub>2</sub>/NO is about 0.93. Figure 9 shows the SCR performances of the Mn-Ce-Ni/TiO<sub>2</sub> catalyst without and with DBD, respectively. At 50 °C, the NO<sub>x</sub> conversion achieved

with two-stage system reaches 80%, indicating that the NO<sub>x</sub> conversion achieved with t two-stage system is higher than that achieved with the catalyst alone by 20%. When temperature is increased to 100 °C, two-stage system reaches 100%. The experimental results indicate that combining Mn-Ce-Ni/TiO<sub>2</sub> with NTP is more effective in reducing NO<sub>x</sub> compared with the catalysis alone at a low temperature. Hence, it can be applied for controlling NO<sub>x</sub> emission from low-loading diesel engine in which the temperature of exhaust gas ranges from 100 to 200 °C (Xie et al. 2012).

As NO reacts with NH<sub>3</sub>, N<sub>2</sub>O is an important by-product. Thus, N<sub>2</sub>O is also measured in this study and the results indicate that the two-stage system produced a lower N<sub>2</sub>O concentration if compared with catalysis alone. At various temperatures tested, the N<sub>2</sub>O concentration generated by two-stage system are all below 30 ppm, while the catalysis-alone generates 90 ppm of N<sub>2</sub>O at 150 °C. The N<sub>2</sub>O concentration of catalyst alone is significantly higher than that generated by the two-stage system. Niu et al. (2016) indicated that N<sub>2</sub>O may be generated from the direct oxidation of NH<sub>3</sub> in the excess O<sub>2</sub> via reaction (2) or NO would react with adsorbed NH<sub>3</sub> on surface of catalyst via reaction (3) at a low temperature (≤150 °C). Also, the N<sub>2</sub>O formation pathway in SCR reaction is the decomposition of intermediate NH<sub>4</sub>NO<sub>3</sub> via reaction (9) (Grossale et al. 2008).



In two-stage system, the plasma can assist the reaction of SCR to induce fast-SCR reaction, achieving a higher NO conversion and a lower N<sub>2</sub>O generation at a temperature ranging

**Fig. 7** The durability test and tolerance of SO<sub>2</sub> and H<sub>2</sub>O<sub>(g)</sub> for SCR reaction

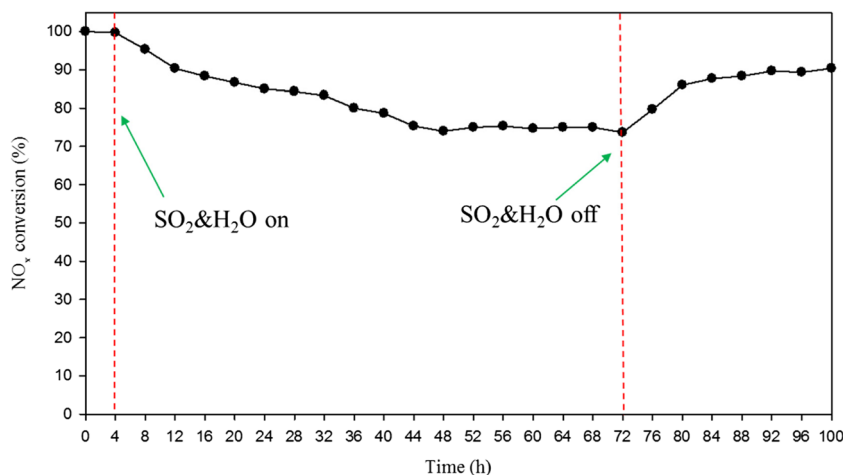
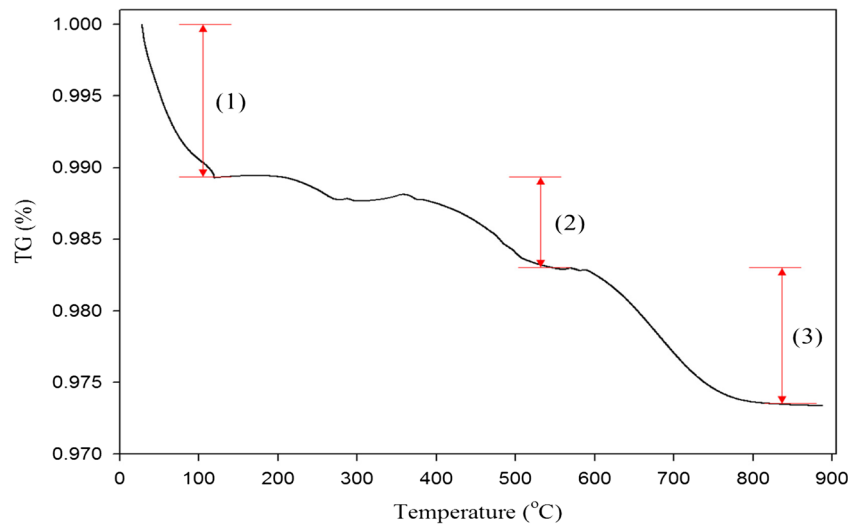




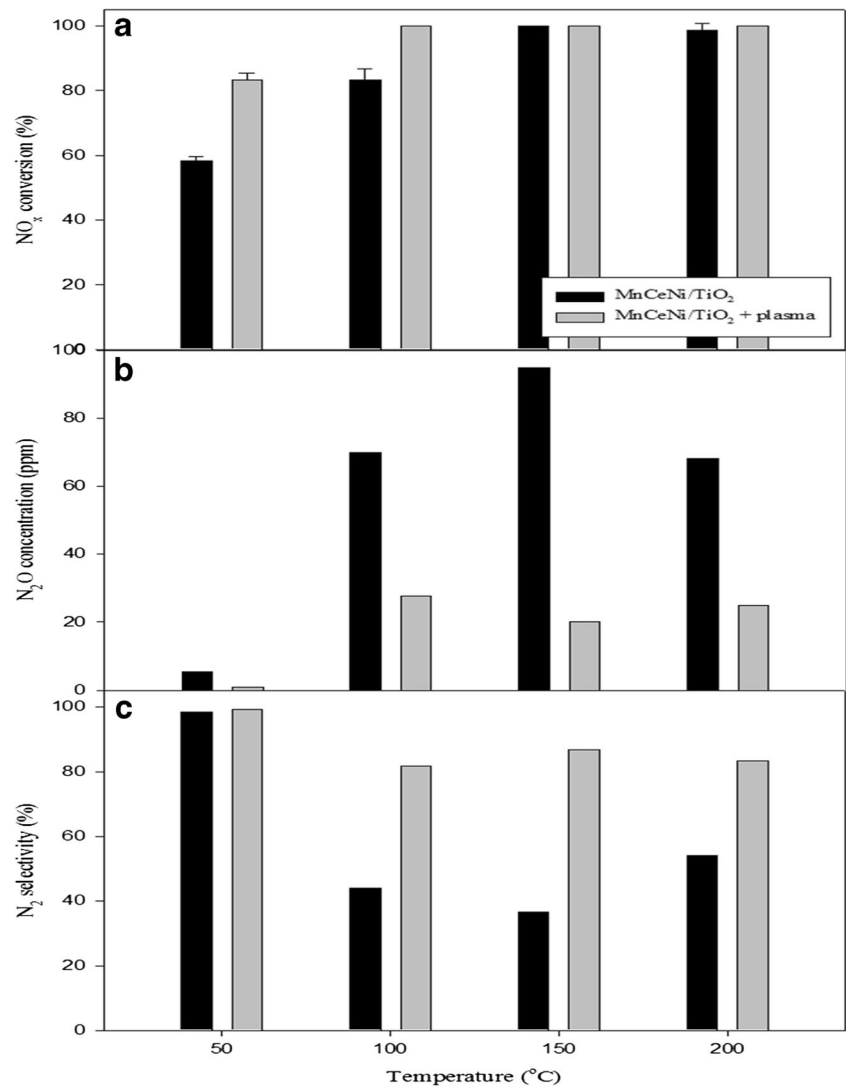
**Fig. 8** TGA curve of used Mn-Ce-Ni/TiO<sub>2</sub> catalyst subjected to H<sub>2</sub>O<sub>(g)</sub> and SO<sub>2</sub>



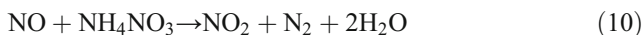
from 50 to 200 °C. The two-stage system can also make SCR reaction more complete than catalyst alone. Moreover, NH<sub>3</sub>

would be effectively consumed by reaction with NO<sub>2</sub> to form NH<sub>4</sub>NO<sub>3</sub>. Subsequently, NH<sub>4</sub>NO<sub>3</sub> is reduced with NO via

**Fig. 9** Comparison of MnCeNi/TiO<sub>2</sub> alone (■) and MnCeNi/TiO<sub>2</sub> + plasma (▨), **a** NO<sub>x</sub> conversion, **b** N<sub>2</sub>O concentration, and **c** N<sub>2</sub> selectivity (300 ppm NO, 300 ppm NH<sub>3</sub>, 10% O<sub>2</sub>, applied voltage: 15.5 kV, frequency: 10 kHz and packed with glass beads)



reaction (10) to inhibit N<sub>2</sub>O formation. In addition, N<sub>2</sub> selectivity of the two-stage system is higher than that of catalyst alone at a temperature range of 50–200 °C because two-stage system generates a lower N<sub>2</sub>O concentration if compared with the catalyst-alone.



### Effect of gas composition on two-stage system

In order to understand the effect of gas composition on the ratio of NO<sub>2</sub>/NO, Fig. 10a–c shows the variation of NO<sub>2</sub>/NO ratio with different gas compositions. The complicated gas compositions are added (including 10% CO<sub>2</sub>, 0.5% CO, and 300 ppm C<sub>2</sub>H<sub>4</sub>) individually, for test. The concentrations of different compositions are chosen based on typical exhaust of diesel engine. As shown in Fig. 10, the NO<sub>2</sub>/NO ratio still can reach 1 for different gas compositions. With the existence of 300 ppm C<sub>2</sub>H<sub>4</sub>, 0.5% CO, and 10% CO<sub>2</sub>, the applied voltage needed to achieve NO<sub>2</sub>/NO = 1 increases to 16.5, 16.5, and 17.5 kV, respectively, if compared with the NO + O<sub>2</sub> only. The gas composition with CO<sub>2</sub> has the most effect on the NO<sub>2</sub>/NO ratio because the concentration of CO<sub>2</sub> is the highest than

others. In addition, CO<sub>2</sub> belongs to electronegative characteristic gas which further forms negative ions such as CO<sub>2</sub><sup>-</sup> to inhibit gas discharge. Generally, existence of electronegative characteristic gas may consume energetic electron in NTP system, resulting in the reduction of discharge performance and a lower ratio of NO<sub>2</sub>/NO. Figure 10d shows that the variation of NO<sub>2</sub>/NO ratio with applied voltage when C<sub>2</sub>H<sub>4</sub>, CO, CO<sub>2</sub>, SO<sub>2</sub>, and H<sub>2</sub>O are present in the flue gas simultaneously. Obviously, the applied voltage has to be increased raise from 15.5 to 18 kV to achieve the fast-SCR condition (NO<sub>2</sub>/NO ≈ 1).

To evaluate the performance of two-stage system to reduce NO<sub>x</sub> to N<sub>2</sub> with complicated gas compositions, the reaction condition is as follows: 300 ppm NO, 300 ppm NH<sub>3</sub>, 300 ppm C<sub>2</sub>H<sub>4</sub>, 0.5% CO, 10% CO<sub>2</sub>, 2% H<sub>2</sub>O<sub>(g)</sub>, and 100 ppm SO<sub>2</sub>. Results indicate that 300 ppm NO in complicated gas compositions could be converted into 156 ppm NO and 152 ppm NO<sub>2</sub> with the applied voltage of 18 kV and frequency of 10 kHz (as presented in Fig. 10d). As shown in Fig. 11, the NO<sub>x</sub> reduction performance reveals an increased trend with increasing temperature and NO<sub>x</sub> conversion reaches 90% at 100 °C. The two-stage system of this study shows better performance for SCR process if compared with literature (as summarize at Table 4).

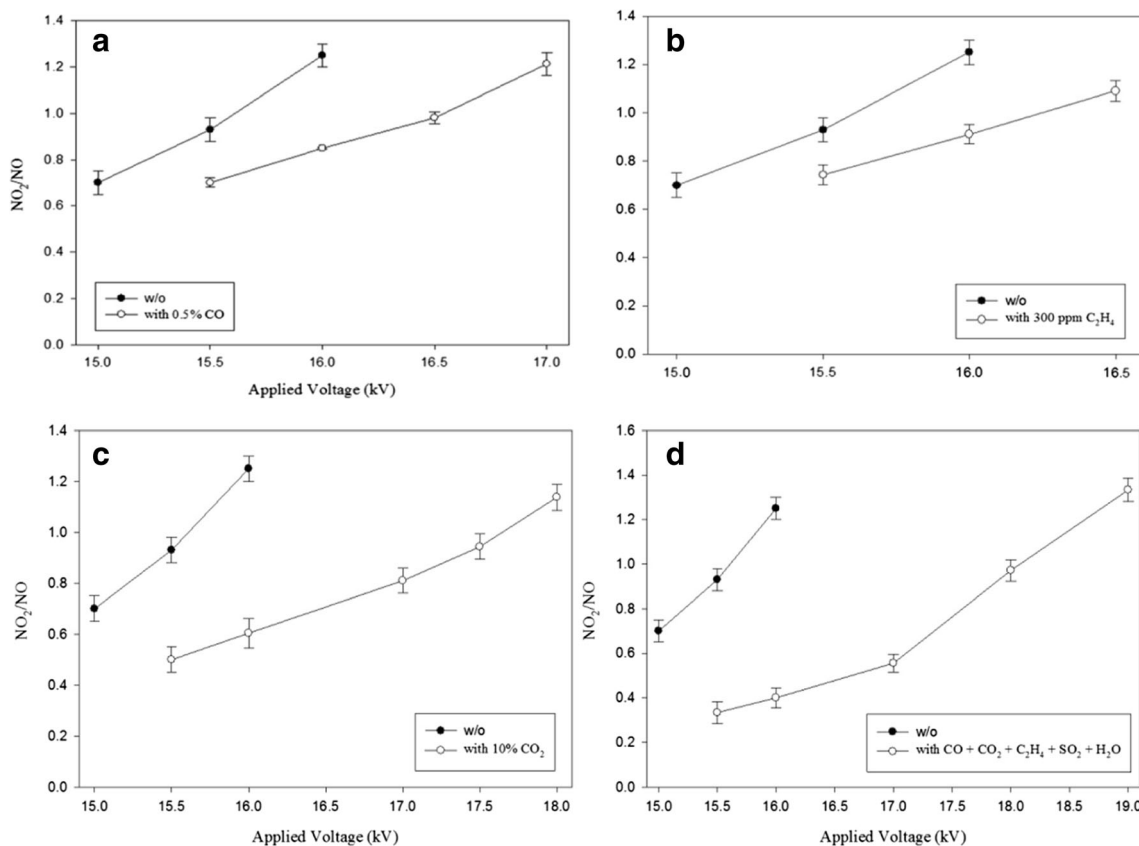


**Fig. 10** Variation of NO<sub>2</sub>/NO with different gas composition **a** NO + O<sub>2</sub> + CO, **b** NO + O<sub>2</sub> + C<sub>2</sub>H<sub>4</sub>, **c** NO + O<sub>2</sub> + CO<sub>2</sub>, **d** NO + O<sub>2</sub> + CO + CO<sub>2</sub> + C<sub>2</sub>H<sub>4</sub> + SO<sub>2</sub> + H<sub>2</sub>O

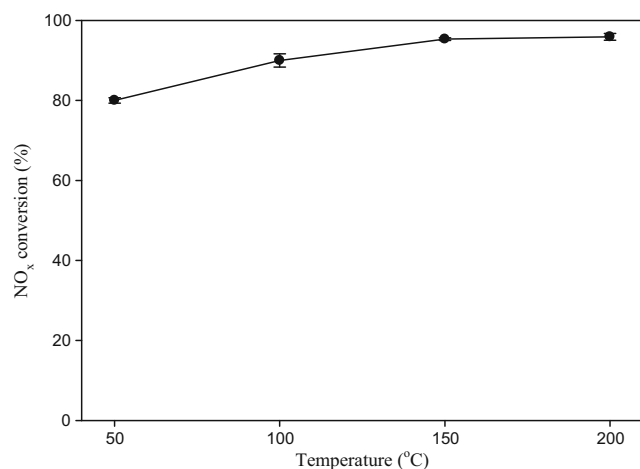


**Fig. 11** Dependence of NO<sub>x</sub> reduction activity on temperature of two-stage system

In addition, it is found that SO<sub>2</sub> concentration is reduced from 100 to 63 ppm as the gases pass through the NTP reactor, and it may be oxidized into SO<sub>3</sub> or H<sub>2</sub>SO<sub>4</sub> by O, OH, or O<sub>3</sub>. Relevant study indicated that the removal process of SO<sub>2</sub> involves oxidation of SO<sub>2</sub> by O, OH, and O<sub>3</sub>, forming SO<sub>3</sub> and H<sub>2</sub>SO<sub>4</sub> in the NTP system (Obradović et al. 2011). The results indicate that NO<sub>x</sub> conversion reaches 95% at 150 °C by two-stage system and it has a good tolerance for H<sub>2</sub>O<sub>(g)</sub> and SO<sub>2</sub> if compared with catalyst-alone. In the two-stage system, NTP system plays an essential role which can effectively oxidize NO to NO<sub>2</sub> for fast-SCR process. Goo et al. (2007) use V<sub>2</sub>O<sub>5</sub>-WO<sub>3</sub>-MnO<sub>2</sub>/TiO<sub>2</sub> with NH<sub>3</sub> as a reducing agent to conduct conventional SCR and fast-SCR for NO removal with the temperature ranging from 200 to 400 °C. The results indicate that fast-SCR has better tolerance for H<sub>2</sub>O<sub>(g)</sub> if compared with conventional SCR. They suggest that the effect of water presence is marginal due to high reaction rate of fast SCR (Goo et al. 2007). In addition, they point out that >90% conversion could be achieved with fast-SCR (with V<sub>2</sub>O<sub>5</sub>-WO<sub>3</sub>-MnO<sub>2</sub>/TiO<sub>2</sub> as catalyst) in the presence of 8% H<sub>2</sub>O<sub>(g)</sub> and 100 ppm SO<sub>2</sub> at 200 °C. Based on literature and the results obtained, it is speculated that fast-SCR has better NO conversion in the

presence of H<sub>2</sub>O<sub>(g)</sub> and SO<sub>2</sub> due to high reaction rate. Also, addition of another reducing agent (C<sub>2</sub>H<sub>4</sub>) in simulated gas streams may help increase NO conversion. These results indicate that the two-stage system has a high NO<sub>x</sub> conversion at a low temperature, and it can operate not only at simple gas composition but also complicated gas condition. The two-stage plasma catalysis system has good potential to improve the activity of NO reduction at a low temperature.

## Conclusions

Conventional SCR process still faces some challenges, for example, it needs to be operated within the temperature range of 250–350 °C for high efficiency. SCR catalyst suffers from deactivation, because conventional SCR process is typically installed before dust removal equipment and flue gas desulfurization (FGD) due to temperature limit. In addition, conventional SCR process cannot be applied for effective removal of NO<sub>x</sub> from diesel engine exhaust due to its low temperature (100–200 °C). In this study, NTP and Mn-based catalyst are combined to form a two-stage system for NO reduction. First, three Mn-based catalysts including Mn-Ce/TiO<sub>2</sub>, Mn-Ce-Ni/TiO<sub>2</sub>, and Mn-Ce-Cu/TiO<sub>2</sub> are evaluated for SCR performance. Experimental results indicate that Mn-Ce-Ni/TiO<sub>2</sub> owns the best activity for SCR reaction among three Mn-based catalysts prepared. However, Mn-Ce-Ni/TiO<sub>2</sub> still needs to be operated at 150 °C for 100% NO<sub>x</sub> conversion, and it also generates significant N<sub>2</sub>O. Further, NTP is placed upstream of SCR system to transform part of NO into NO<sub>2</sub> for achieving fast-SCR. Results indicate that the NO<sub>x</sub> conversion and N<sub>2</sub> selectivity achieved can reach 100 and 80%, respectively, and the N<sub>2</sub>O concentration measured is lower than that of catalysis alone at 100 °C. The condition of NO<sub>2</sub>/NO = 1 can be achieved for fast SCR by applying appropriate voltage with plasma system. This study demonstrates that combining Mn-based catalysts with NTP can successfully achieve fast SCR reaction to reduce NO<sub>x</sub> to N<sub>2</sub>, with a high efficiency and N<sub>2</sub> selectivity. This study indicates that plasma-assisted system

**Table 4** Comparison of performance of the NTP enhanced SCR with literature

| Catalysts  | Plasma type | Voltage (kV) | Frequency (kHz) | Reducing agent                | NO conc. (ppm) | SCR Temp. (°C) | Removal efficiency (%) | Reference               |
|--|-------------|--------------|-----------------|-------------------------------|----------------|----------------|------------------------|-------------------------|
| Mn-Ce-Ni/TiO <sub>2</sub>  | DBD         | 15.5         | 10              | NH <sub>3</sub>               | 300            | 150            | >99                    | This study              |
| H-mordenite  | DBD         | 20           | –               | NH <sub>3</sub>               | 500            | 160            | 76                     | Miessner et al. (2002)  |
| V <sub>2</sub> O <sub>5</sub> -WO <sub>3</sub> /TiO <sub>2</sub> | DBD         | 10           | 1               | NH <sub>3</sub>               | 500            | 200            | >99                    | Bröer and Hammer (2000) |
| Co-HZSM-5  | DBD         | –            | –               | C <sub>2</sub> H <sub>2</sub> | 500            | 300            | 90                     | Niu et al. (2006)       |
| NH <sub>4</sub> -mordenite                                       | DBD         | –            | –               | C <sub>3</sub> H <sub>6</sub> | 500            | 200            | >100                   | Chae (2003)             |
| BaY + CuY  | –           | 16           | –               | C <sub>x</sub> H <sub>y</sub> | 182            | 200            | 95                     | Cho et al. (2012)       |

can improve the performance of SCR catalyst, and it has high performance at a low temperature ( $\leq 200$  °C).

## Nomenclature

### Item

10% wt. Mn-Ce/TiO<sub>2</sub> = Mn-Ce/TiO<sub>2</sub>

10% wt. Mn-Ce-Ni/TiO<sub>2</sub> = Mn-Ce-Ni/TiO<sub>2</sub>

10% wt. Mn-Ce-Cu/TiO<sub>2</sub> = Mn-Ce-Cu/TiO<sub>2</sub>

Dielectric barrier discharge = DBD

Nonthermal plasma = NTP

Selective catalytic reduction = SCR

SCR system + NTP = two-stage system

## References

- Boningari T, Ettireddy PR, Somogyvari A, Liu Y, Vorontsov A, McDonald CA, Smirniotis PG (2015) Influence of elevated surface texture hydrated titania on Ce-doped Mn/TiO<sub>2</sub> catalysts for the low-temperature SCR of NO<sub>x</sub> under oxygen-rich conditions. *J Catal* 325: 145–155
- Bocuzzi F, Chiorino A, Martra G, Gargano M, Ravasio N, Carrozzini B (1997) Preparation, characterization, and activity of Cu/TiO<sub>2</sub> catalysts. I. Influence of the preparation method on the dispersion of copper in Cu/TiO<sub>2</sub>. *J Catal* 165:129–139
- Bröer S, Hammer T (2000) Selective catalytic reduction of nitrogen oxides by combining a non-thermal plasma and a V<sub>2</sub>O<sub>5</sub>-WO<sub>3</sub>/TiO<sub>2</sub> catalyst. *Appl Catal B Environ* 28:101–111
- Cao F, Su S, Xiang J, Wang P, Hu S, Sun L, Zhang A (2015) The activity and mechanism study of Fe-Mn-Ce/γ-Al<sub>2</sub>O<sub>3</sub> catalyst for low temperature selective catalytic reduction of NO with NH<sub>3</sub>. *Fuel* 139: 232–239
- Chang H, Li J, Yuan J, Chen L, Dai Y, Arandiyani H, Xu J, Hao J (2013) Ge, Mn-doped CeO<sub>2</sub>-WO<sub>3</sub> catalysts for NH<sub>3</sub>-SCR of NO<sub>x</sub>: effects of SO<sub>2</sub> and H<sub>2</sub> regeneration. *Catal Today* 201:139–144
- Chae JO (2003) Non-thermal plasma for diesel exhaust treatment. *J Electrostat* 57:251–262
- Chen H-Y, Wei Z, Kollar M, Gao F, Wang Y, Szanyi J, Peden CHF (2016) NO oxidation on zeolite supported Cu catalysts: formation and reactivity of surface nitrates. *Catal Today* 267:17–27
- Cho BK, Lee J-H, Crellin CC, Olson KL, Hilden DL, Kim MK, Kim PS, Heo I, Oh SH, Nam I-S (2012) Selective catalytic reduction of NO<sub>x</sub> by diesel fuel: plasma-assisted HC/SCR system. *Catal Today* 191: 20–24
- Choi B, Woo S-M (2015) Numerical analysis of the optimum heating pipe to melt frozen urea-water-solution of a diesel urea-SCR system. *Appl Therm Eng* 89:860–870
- Cimino S, Lisi L, Tortorelli M (2016) Low temperature SCR on supported MnO<sub>x</sub> catalysts for marine exhaust gas cleaning: effect of KCl poisoning. *Chem Eng J* 283:223–230
- Fang D, Xie J, Hu H, Yang H, He F, Fu Z (2015) Identification of MnO<sub>x</sub> species and Mn valence states in MnO<sub>x</sub>/TiO<sub>2</sub> catalysts for low temperature SCR. *Chem Eng J* 271:23–30
- Feng T, Lü L (2015) The characteristics of ammonia storage and the development of model-based control for diesel engine urea-SCR system. *J Ind Eng Chem* 28:97–109
- Grossale A, Nova I, Tronconi E, Chatterjee D, Weibel M (2008) The chemistry of the NO/NO<sub>2</sub>-NH<sub>3</sub> “fast” SCR reaction over Fe-ZSM5 investigated by transient reaction analysis. *J Catal* 256:312–322
- Goo JH, Irfan MF, Kim SD, Hong SC (2007) Effects of NO<sub>2</sub> and SO<sub>2</sub> on selective catalytic reduction of nitrogen oxides by ammonia. *Chemosphere* 67:718–723
- Huang L, Wang X, Yao S, Jiang B, Chen X, Wang X (2016) Cu-Mn bimetal ion-exchanged SAPO-34 as an active SCR catalyst for removal of NO<sub>x</sub> from diesel engine exhausts. *Catal Commun* 81:54–57
- Iwasaki M, Shinjoh H (2010) A comparative study of “standard”, “fast” and “NO<sub>2</sub>” SCR reactions over Fe/zeolite catalyst. *Appl Catal A Gen* 390:71–77
- Jōgi I, Erme K, Raud J, Laan M (2016) Oxidation of NO by ozone in the presence of TiO<sub>2</sub> catalyst. *Fuel* 173:45–51
- Jin R, Liu Y, Wang Y, Cen W, Wu Z, Wang H, Weng X (2014) The role of cerium in the improved SO<sub>2</sub> tolerance for NO reduction with NH<sub>3</sub> over Mn-Ce/TiO<sub>2</sub> catalyst at low temperature. *Appl Catal B Environ* 148-149:582–588
- Jun L, Liwei J, Weiyang J, Feng X, Jiaming W (2015) Effects of Ce-doping on the structure and NH<sub>3</sub>-SCR activity of Fe/Beta catalyst. *Rare Metal Mater Eng* 44:1612–1616
- Kang M, Kim DJ, Park ED, Kim JM, Yie JE, Kim SH, Hope-Weeks L, Eyring EM (2006a) Two-stage catalyst system for selective catalytic reduction of NO<sub>x</sub> by NH<sub>3</sub> at low temperatures. *Appl Catal B Environ* 68:21–27
- Kang M, Yeon TH, Park ED, Yie JE, Kim JM (2006b) Novel MnO<sub>x</sub> catalysts for NO reduction at low temperature with ammonia. *Catal Lett* 106:77–80
- Koebel M, Elsener M, Madia G (2001) Reaction pathways in the selective catalytic reduction process with NO and NO<sub>2</sub> at low temperatures. *Ind Eng Chem Res* 40:52–59
- Koebel M, Madia G, Raimondi F, Wokaun A (2002) Enhanced reoxidation of vanadia by NO<sub>2</sub> in the fast SCR reaction. *J Catal* 209:159–165
- Kwon DW, Nam KB, Hong SC (2015) The role of ceria on the activity and SO<sub>2</sub> resistance of catalysts for the selective catalytic reduction of NO<sub>x</sub> by NH<sub>3</sub>. *Appl Catal B Environ* 166–167:37–44
- Liu J, Li X, Zhao Q, Ke J, Xiao H, Lv X, Liu S, Tadé M, Wang S (2017) Mechanistic investigation of the enhanced NH<sub>3</sub>-SCR on cobalt-decorated Ce-Ti mixed oxide: in situ FTIR analysis for structure-activity correlation. *Appl Catal B Environ* 200:297–308
- Ma Z, Wu X, Feng Y, Si Z, Weng D (2015) Effects of WO<sub>3</sub> doping on stability and N<sub>2</sub>O escape of MnO<sub>x</sub>-CeO<sub>2</sub> mixed oxides as a low-temperature SCR catalyst. *Catal Commun* 69:188–192
- Madia G, Koebel M, Elsener M, Wokaun A (2002) The effect of an oxidation pre-catalyst on the NO<sub>x</sub> reduction by ammonia SCR. *Ind Eng Chem Res* 41:3512–3517
- Miessner H, Francke K-P, Rudolph R, Hammer T (2002) NO<sub>x</sub> removal in excess oxygen by plasma-enhanced selective catalytic reduction. *Catal Today* 75:325–330
- Niu Y, Shang T, Hui S, Zhang X, Lei Y, Lv Y, Wang S (2016) Synergistic removal of NO and N<sub>2</sub>O in low-temperature SCR process with MnO<sub>x</sub>/Ti based catalyst doped with Ce and V. *Fuel* 185:316–322
- Niu J, Yang X, Zhu A, Shi L, Sun Q, Xu Y, Shi C (2006) Plasma-assisted selective catalytic reduction of NO<sub>x</sub> by C<sub>2</sub>H<sub>2</sub> over co-HZSM-5 catalyst. *Catal Commun* 7:297–301
- Obradović BM, Sretenović GB, Kuraica MM (2011) A dual-use of DBD plasma for simultaneous NO<sub>x</sub> and SO<sub>2</sub> removal from coal-combustion flue gas. *J Hazard Mater* 185:1280–1286
- Patil BS, Cherkasov N, Lang J, Ibhaddon AO, Hessel V, Wang Q (2016) Low temperature plasma-catalytic NO<sub>x</sub> synthesis in a packed DBD reactor: effect of support materials and supported active metal oxides. *Appl Catal B Environ* 194:123–133
- Peña DA, Uphade BS, Smirniotis PG (2004) TiO<sub>2</sub>-supported metal oxide catalysts for low-temperature selective catalytic reduction of NO

- with NH<sub>3</sub>: I. Evaluation and characterization of first row transition metals *Journal of Catalysis* 221:421–431
- Peng Y, Li K, Li J (2013) Identification of the active sites on CeO<sub>2</sub>–WO<sub>3</sub> catalysts for SCR of NO<sub>x</sub> with NH<sub>3</sub>: an in situ IR and Raman spectroscopy study. *Appl Catal B Environ* 140–141:483–492
- Phil HH, Reddy MP, Kumar PA, Ju LK, Hyo JS (2008) SO<sub>2</sub> resistant antimony promoted V<sub>2</sub>O<sub>5</sub>/TiO<sub>2</sub> catalyst for NH<sub>3</sub>-SCR of NO<sub>x</sub> at low temperatures. *Appl Catal B Environ* 78:301–308
- Putluru SSR, Schill L, Jensen AD, Siret B, Tabaries F, Fehrmann R (2015) Mn/TiO<sub>2</sub> and Mn–Fe/TiO<sub>2</sub> catalysts synthesized by deposition precipitation—promising for selective catalytic reduction of NO with NH<sub>3</sub> at low temperatures. *Appl Catal B Environ* 165:628–635
- Shaju KM, Subba Rao GV, Chowdari BVR (2002) Performance of layered li(Ni<sub>1/3</sub>Co<sub>1/3</sub>Mn<sub>1/3</sub>) O<sub>2</sub> as cathode for li-ion batteries. *Electrochim Acta* 48:145–151
- Shen B, Wang Y, Wang F, Liu T (2014) The effect of Ce–Zr on NH<sub>3</sub>-SCR activity over MnO<sub>x(0.6)</sub>/Ce<sub>0.5</sub>Zr<sub>0.5</sub>O<sub>2</sub> at low temperature. *Chem Eng J* 236:171–180
- Shu Y, Aikebaier T, Quan X, Chen S, Yu H (2014) Selective catalytic reaction of NO<sub>x</sub> with NH<sub>3</sub> over Ce–Fe/TiO<sub>2</sub>-loaded wire-mesh honeycomb: resistance to SO<sub>2</sub> poisoning. *Appl Catal B Environ* 150–151:630–635
- Tang X, Hao J, Xu W, Li J (2007) Low temperature selective catalytic reduction of NO<sub>x</sub> with NH<sub>3</sub> over amorphous MnO<sub>x</sub> catalysts prepared by three methods. *Catal Commun* 8:329–334
- Thirupathi B, Smirniotis PG (2011a) Co-doping a metal (Cr, Fe, Co, Ni, Cu, Zn, Ce, and Zr) on Mn/TiO<sub>2</sub> catalyst and its effect on the selective reduction of NO with NH<sub>3</sub> at low-temperatures. *Appl Catal B Environ* 110:195–206
- Thirupathi B, Smirniotis PG (2011b) Effect of nickel as dopant in Mn/TiO<sub>2</sub> catalysts for the low-temperature selective reduction of NO with NH<sub>3</sub>. *Catal Lett* 141:1399
- Tran DN, Aardahl CL, Rappe KG, Park PW, Boyer CL (2004) Reduction of NO<sub>x</sub> by plasma-facilitated catalysis over in-doped  $\gamma$ -alumina. *Appl Catal B Environ* 48:155–164
- Wan Y, Zhao W, Tang Y, Li L, Wang H, Cui Y, Gu J, Li Y, Shi J (2014) Ni–Mn bi-metal oxide catalysts for the low temperature SCR removal of NO with NH<sub>3</sub>. *Appl Catal B Environ* 148–149:114–122
- Wang X, Li X, Zhao Q, Sun W, Tade M, Liu S (2016) Improved activity of W-modified MnO<sub>x</sub>-TiO<sub>2</sub> catalysts for the selective catalytic reduction of NO with NH<sub>3</sub>. *Chem Eng J* 288:216–222
- Wu Z, Jiang B, Liu Y, Zhao W, Guan B (2007) Experimental study on a low-temperature SCR catalyst based on MnO<sub>x</sub>/TiO<sub>2</sub> prepared by sol–gel method. *J Hazard Mater* 145:488–494
- Xie J, Fang D, He F, Chen J, Fu Z, Chen X (2012) Performance and mechanism about MnO<sub>x</sub> species included in MnO<sub>x</sub>/TiO<sub>2</sub> catalysts for SCR at low temperature. *Catal Commun* 28:77–81
- Yang N-z, Guo R-t, Pan W-g, Q-l C, Wang Q-s, Lu C-z (2016) The promotion effect of Sb on the Na resistance of Mn/TiO<sub>2</sub> catalyst for selective catalytic reduction of NO with NH<sub>3</sub>. *Fuel* 169:87–92
- Yoshida K, Kuwahara T, Kuroki T, Okubo M (2012) Diesel NO<sub>x</sub> aftertreatment by combined process using temperature swing adsorption, NO<sub>x</sub> reduction by nonthermal plasma, and NO<sub>x</sub> recirculation: improvement of the recirculation process. *J Hazard Mater* 231–232:18–25
- Yu J, Guo F, Wang Y, Zhu J, Liu Y, Su F, Gao S, Xu G (2010) Sulfur poisoning resistant mesoporous Mn-base catalyst for low-temperature SCR of NO with NH<sub>3</sub>. *Appl Catal B Environ* 95:160–168
- Zhou A, Yu D, Yang L, Sheng Z (2016) Combined effects Na and SO<sub>2</sub> in flue gas on Mn–Ce/TiO<sub>2</sub> catalyst for low temperature selective catalytic reduction of NO by NH<sub>3</sub> simulated by Na<sub>2</sub>SO<sub>4</sub> doping. *Appl Surf Sci* 378:167–173